UDK 546.46:629.5.017.22
Original scientific article/Izvirni znanstveni članek

ISSN 1580-2949
MTAEC9, 58(2)113(2024)

EFFECT OF OUTPUT VOLTAGE ON AN AZ91D MAGNESIUM ALLOY ROLLED USING AN ELECTRIC PULSE TREATMENT

VPLIV VHODNE NAPETOSTI NA MAGNEZIJEVO ZLITINO VRSTE AZ91D, VALJANE POD VPLIVOM ELEKTRIČNIH IMPULZOV

Jing Feng[1], Yuezhang Zhou[2], Dehua Liu[1], Yong Zhang[3], Guihong Geng[1*]

[1]School of Materials Science and Engineering, North Minzu University, Yinchuan 750021, P.R. China
[2]Beijing Chemical Industry Research Institute Co., Ltd, Beijing 100080, China
[3]State Key Laboratory for Advanced Metals and Materials, University of Science and Technology Beijing, Beijing 100083, China

Prejem rokopisa – received: 2023-07-27; sprejem za objavo – accepted for publication: 2024-01-11

doi:10.17222/mit.2023.960

Magnesium alloys have poor deformation properties at room temperature, and the application of an electric pulse current during deformation can improve the plastic-forming ability. In this study, the electric pulse rolling of AZ91D magnesium alloy specimens has been examined by changing the pulse output voltage. The results demonstrate that the best surface quality and lowest content (8.4 %) of the β-$Mg_{17}Al_{12}$ phase are achieved at an output voltage of 300 V. EBSD tests have revealed the lowest weave strength on {0002} and {1010} at a pulse output voltage of 300 V, as well as the greatest enhancement of twinning. The maximum tensile strength was 165 MPa at an output voltage of 300 V, with a maximum elongation of 4.1 % at an output voltage of 200 V.

Keywords: output voltage; electric pulse rolling; AZ91D magnesium alloy; properties

Zlitine na osnovi magnezija se slabo deformirajo pri sobni temperaturi, vendar uporaba električnih tokovnih impulzov med deformacijo lahko izboljša njihovo sposobnost za plastično preoblikovanje. V tem članku avtorji opisujejo študijo valjanja magnezijeve zlitine vrste AZ91D spodbujeno z električnimi impulzi različno visoke vhodne) napajalne napetosti. Rezultati preizkusov so pokazali, da so avtorji dosegli najboljšo kvaliteto površine in najmanjšo vsebnost (8,4%) intermetalne faze β-$Mg_{17}Al_{12}$ pri napetosti 300V. Preiskave s pomočjo spektrostopije s povratno sipanimi elektroni (EBSD; angl.: electron back scattered dispersion) so pokazale najmanjšo zvojno trdnost na kristalografskih ravninah {0002} in {1010} pri 300V tokovnih impulzih ter največje povečanje dvojčenja. Največja natezna trdnost izbrane zlitin 165 MPa pri napetosti 300 V in maksimalni raztezek zlitine 4,1% so dosegli pri napetosti 200 V.

Ključne besede: zunanja (napajalna) napetost, valjanje pod vplivom električnih impulzov, magnezijeva zlitina vrste AZ91D, lastnosti

1 INTRODUCTION

Magnesium alloys exhibit a high specific strength and stiffness, good electrical and thermal conductivity and electromagnetic shielding properties with excellent casting properties. The use of these alloys as structural parts in automotive, aerospace, electronic products and communication equipment represents wide-ranging applications.[1–3] However, the room-temperature deformation of these alloys is poor, preventing cold rolling, cold stamping and other cold-deformation methods for mass production. Moreover, under hot-forming conditions the magnesium alloy readily undergoes oxidation with associated mold surface friction and wear. There is now an urgent need to develop a new and efficient plastic-forming process for magnesium alloys that can be used in industrial production.

In recent years, researchers have found that the application of a pulse current during the deformation of metal materials can effectively improve the plastic-forming capability, and this phenomenon is termed the "electroplastic effect".[4,5] The use of pulsed currents has now been applied in various plastic-forming processes.[6–9] The pulsed current can reduce flow stress in metallic materials by influencing the movement and proliferation of dislocations.[10–12] Zhou Yizhou et al.[13,14] found that brass and steel produced by cold rolling formed ultrafine grains in a short time after the electric pulse treatment, which substantially improved the overall mechanical properties of the material. In the pulsed current treatment of cold-rolled Cu-Zn alloys, Dai Wenbin et al.[15,16] observed a current induced recrystallization that occurred in a directional manner. Fan et al.[17,18] have performed electrical pulse treatments on magnesium alloys and found that the non-thermal effect of the pulsed current can promote material recovery and recrystallization at a lower temperature. Jeong et al.[19] investigated the tensile deformation of an extruded AZ91 magnesium alloy under the action of a pulsed current by performing standard-tensile in addition to pulsed-tensile experiments at room temperature and 70 °C. The results showed that the $Mg_{17}Al_{12}$ phase was significantly reduced in the tensile specimens treated by an electric pulse when compared to the samples without any electric-pulse treatment. The pulse current promoted

*Corresponding author's e-mail:
gengguihong@nmu.edu.cn (Guihong Geng)

dissolution of the $Mg_{17}Al_{12}$ phase in the extruded AZ91, which improved the overall performance of the alloy. Indhiarto et al.[20] performed unidirectional tensile experiments on AZ31B by applying pulsed currents with different peak-current densities at the same temperature. The results revealed that the ultimate tensile strength decreased with increasing peak-current density, independent of the temperature, demonstrating a non-thermal positive effect of the pulsed current on the tensile properties. Currently, the evolution of the tissue properties of the pulsed-current-induced deformation of magnesium alloys has not been sufficiently studied. There is relatively little research on the electroplasticity of magnesium alloys and the effect of electric pulse on the alloy during processing. This has hampered the application of electric-pulse-rolling magnesium alloy technology.

In this study, the effects of different pulse output voltages on the structure and properties of an AZ91D magnesium alloy rolled using electric pulses have been investigated. The results generated are significant in advancing the electroplasticity of magnesium alloys and the production practice of electric-pulse rolling.

2 EXPERIMENTAL MATERIALS AND METHODS

2.1 Experimental materials

The cast AZ91D magnesium alloy was selected as the test material, and the main components are shown in **Table 1**. Samples were completely annealed at 400 °C for 3h, with air cooling before use. The AZ91D alloy samples were cut into (60×12×3) mm experimental plates using wire cutting.

Table 1: Main components of the AZ91D magnesium alloy

Element	Al	Zn	Mn	Si	Cu	Mg
w/%	9	0.67	0.25	0.05	0.015	Allowance

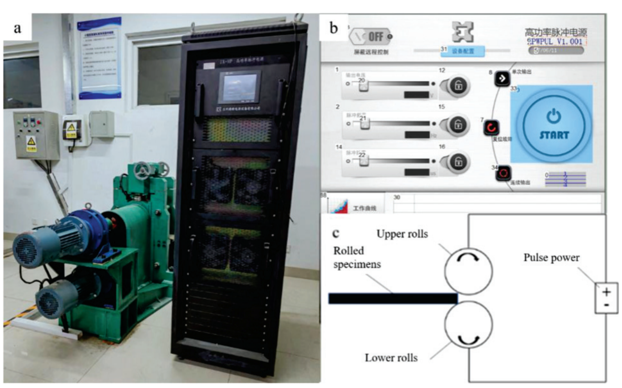

Figure 1: Schematic diagram of the strong-pulse rolling equipment and the working principles: a) shows an image of the strong-pulse rolling equipment, b) illustrates the strong-pulse power control panel, c) is a schematic representation of the electric-pulse rolling process

2.2 Experimental methods

The experiments were conducted at five output voltages (0 V (no electrical pulse applied), 100 V, 200 V, 300 V and 400 V) for the single-pass, large-depression (20 %) electric-pulse rolling of AZ91D; the rolling parameters are shown in **Table 2**. An infrared temperature gun was used to measure the temperature of the sample when it entered and exited the roll, and an oscilloscope was used to monitor the output current of the pulse power supply. The microstructure and mechanical properties of the AZ91D samples rolled under the five different output-voltage conditions were analyzed.

The experimental tests used strong-pulsed-current rolling equipment developed in our laboratory, and is composed of two parts: rolling equipment and a strong-pulsed-power supply. Pressure sensors on the rolls displayed the pressure between the upper and lower rolls in real time; the strong-pulse rolling equipment and the working principles are illustrated schematically in **Figure 1**.

Table 2: Rolling parameters

Sample number	Voltage (V)	Frequency (Hz)	Pulse Width (μs)	Current Density (A/mm^2)	Roll-in temperature (°C)	Roll-out temperature (°C)
EP0	0	–	–	–	81	27
EP1	100	600	20	69	77	25
EP2	200	600	20	342	77	26
EP3	300	600	20	364	79	25
EP4	400	600	20	410	78	25

2.3 Analytical Testing

Analysis of the fracture morphology of the electro-pulsed rolled AZ91D employed a ZEISS-Vert.A1 inverted metallurgical microscope. The sample microstructure was evaluated using a ZEISS Sigma 500 thermal field-emission scanning electron microscope equipped with an X-ray energy spectrum analyzer (EDS) and electron-backscatter diffraction (EBSD) at an accelerating voltage of 15 kV and an optical diaphragm of 60 μm. An HXD-1000TM microhardness tester was employed with an experimental load of 4.9 N and a load time of 15 s. The CMT5305 microcomputer-controlled electronic universal testing machine was used for room-temperature tensile performance testing.

3 RESULTS AND DISCUSSION

3.1 Effect of output voltage on the surface morphology of AZ91D magnesium alloy rolled by an electric-pulse treatment

The sample morphology of the AZ91D rolled by an electric-pulse treatment at different output voltages is illustrated in **Figure 2**. It can be seen that the samples EP4 all have fewer surface cracks than EP0, which was not subjected to electric-pulse rolling. The EP0 sample ex-

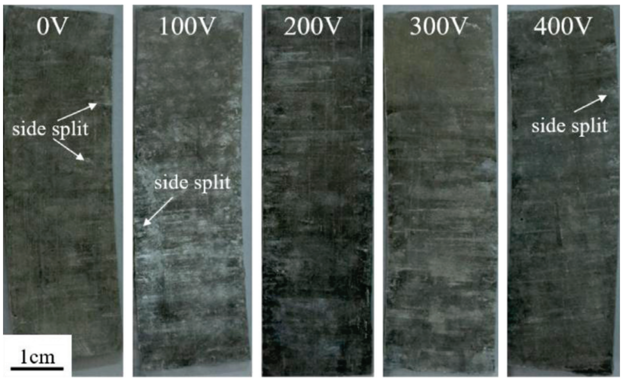

Figure 2: Sample morphology of AZ91D magnesium alloy rolled by an electric-pulse treatment at different output voltages

hibited more fine cracks at the edges with evidence of bending after rolling. There were no obvious defects such as surface cracks on the surface of EP2 and EP3 samples, where the output voltage was 200 V and 300 V, respectively. A small number of edge cracks appeared on the surface of the EP4 sample rolled by an electric pulse at an output voltage of 400 V.

As the dense hexagonal crystal structure of the EP0 alloy is resistant to opening, cracks appeared during the rolling process. The EP1-3 samples treated with electric pulses of 100–300 V exhibited a gradual reduction in surface cracking with an improved plastic-forming capability. This can be attributed to the effects of the energy and magnetic field generated by the pulsed current on the dislocation debonding and debonding rate. The induction magnetic field can alter the binding energy of the dislocation and the paramagnetic phase from the S state (single state) to the T state (triple state), so that the dislocation is not entangled but can readily detach from the center of the pegging. This effect facilitates the sliding of dislocations on different crystal surfaces, which minimizes or eliminates the surface-crack formation. When the output voltage was 400 V in the case of EP4, the appearance of sample cracks during rolling may be due to further dislocation slippage causing dislocation proliferation that results in process hardening.[21]

3.2 Effect of output voltage on the electric-pulse rolling of the β-$Mg_{17}Al_{12}$ phase of AZ91D magnesium alloy

The SEM images of the AZ91D after rolling by electric pulses with different output voltages are shown in **Figure 3**. It can be seen that the β-$Mg_{17}Al_{12}$ phase in the EP0 sample is distributed in the α-Mg matrix as a coarse, irregular, skeleton-like formation grid, with evidence of significant crack formation. The morphology of the β-$Mg_{17}Al_{12}$ phase in EP1 is similar to that of the EP0 sample, but the surface cracks were significantly reduced. The β-$Mg_{17}Al_{12}$ phase in the EP2 and EP3 samples changed from a coarse irregular skeletal arrangement to fine, worm-like formations with a secondary presence of flakes, and no obvious surface cracks. In the case of EP4, the β-$Mg_{17}Al_{12}$ phase exhibits a coarseness and irregular skeletal morphology, but no obvious crack formation.

The content of the β-$Mg_{17}Al_{12}$ phase in the AZ91D was estimated from its area share in the SEM images, and the results of the calculations are presented in **Figure 4**. It can be seen that the β-$Mg_{17}Al_{12}$ phase content decreased from 11.3 % to 8.4 % with increasing output voltage from 0 V to 300 V. At a voltage of 400 V, the β-$Mg_{17}Al_{12}$ content increased to 10.5%. In the operation of the rolling process at an output voltage of 0V-300V, the introduction of the pulse current caused a dissolution of the β-$Mg_{17}Al_{12}$ phase at a temperature lower than its

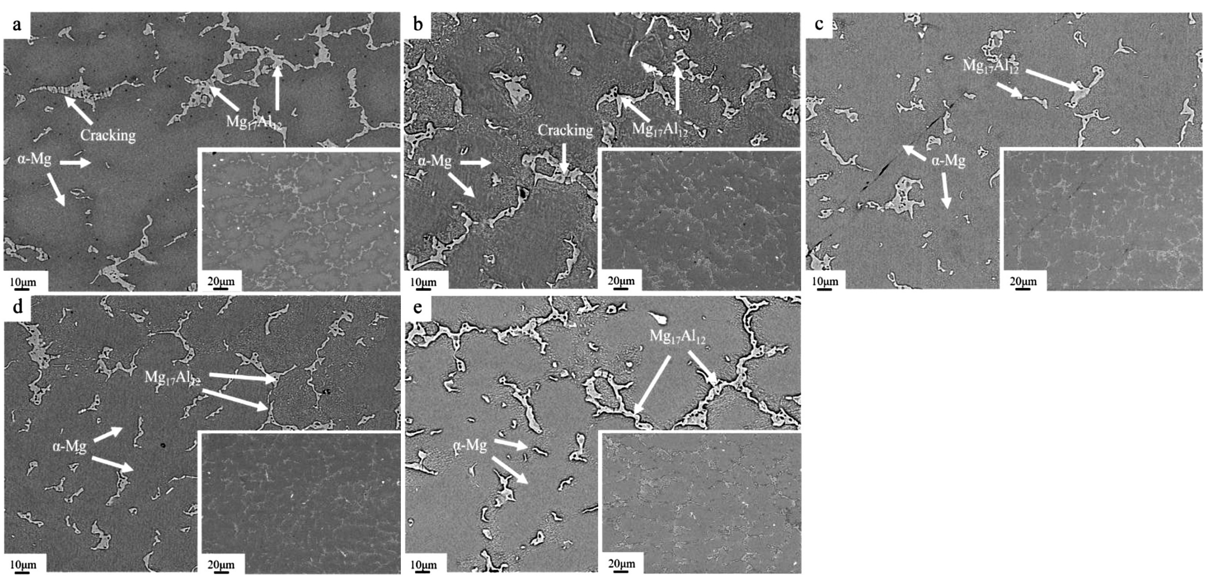

Figure 3: SEM images of AZ91D magnesium alloy rolled by electric pulse treatment at different output voltages: a) EP0 sample (0 V), b) EP1 sample (100 V), c) EP2 sample (200 V), d) EP3 sample (300 V), e) EP4 sample (400 V)

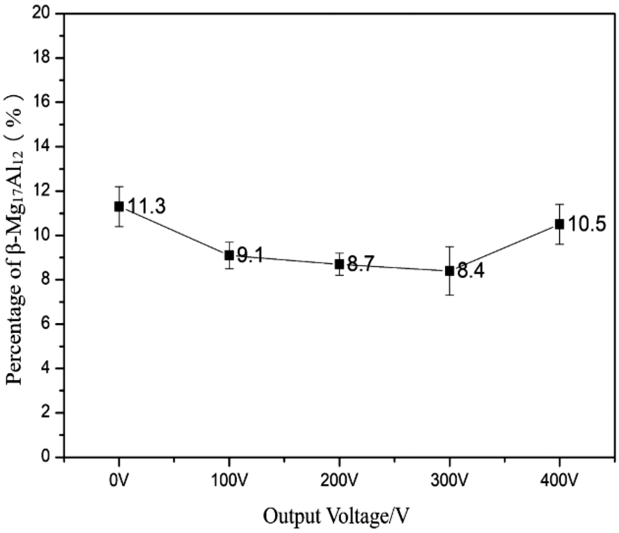

Figure 4: Content of the β-$Mg_{17}Al_{12}$ phase in AZ91D magnesium alloy rolled by electric-pulse treatment at different output voltages

dissolution temperature (ca. 420°C). This can be attributed to a "thermal effect + non-thermal effect" synergism, where the dissolved β-$Mg_{17}Al_{12}$ phase is dispersed in the AZ91D matrix. When the voltage was increased to 400 V, the solid solution in the Mg matrix reached an upper limit due to the pulse-voltage energy which impeded β-$Mg_{17}Al_{12}$ dissolution, resulting in a gradual coarsening.[22]

3.3 *Effect of output voltage on the weave of AZ91D magnesium alloy rolled by electric pulse treatment*

The EBSD images and polar diagrams for the electric-pulse rolling of the AZ91D magnesium alloy at different output voltages are shown in **Figure 5**. It can be seen that the weave strength of the EP0-EP3 samples on {0002} and $\{10\bar{1}0\}$ gradually decreased in the output-voltage range 0–300 V. The weave strength on {0002} decreased from 10.23 in EP0 to 4.98 in EP3. The weave strength on $\{10\bar{1}0\}$ decreased from 4.03 for EP0 to 1.88 for EP3. On increasing the output voltage to 400 V, the weave intensity on {0002} and $\{10\bar{1}0\}$ increased. At an output voltage of 0–300 V, the pulse current resulted in a random grain orientation. This response can optimize the dislocation-slip mechanism configuration and lower the stress concentration in adjacent grains during the forming process, enhancing the strain coordi-

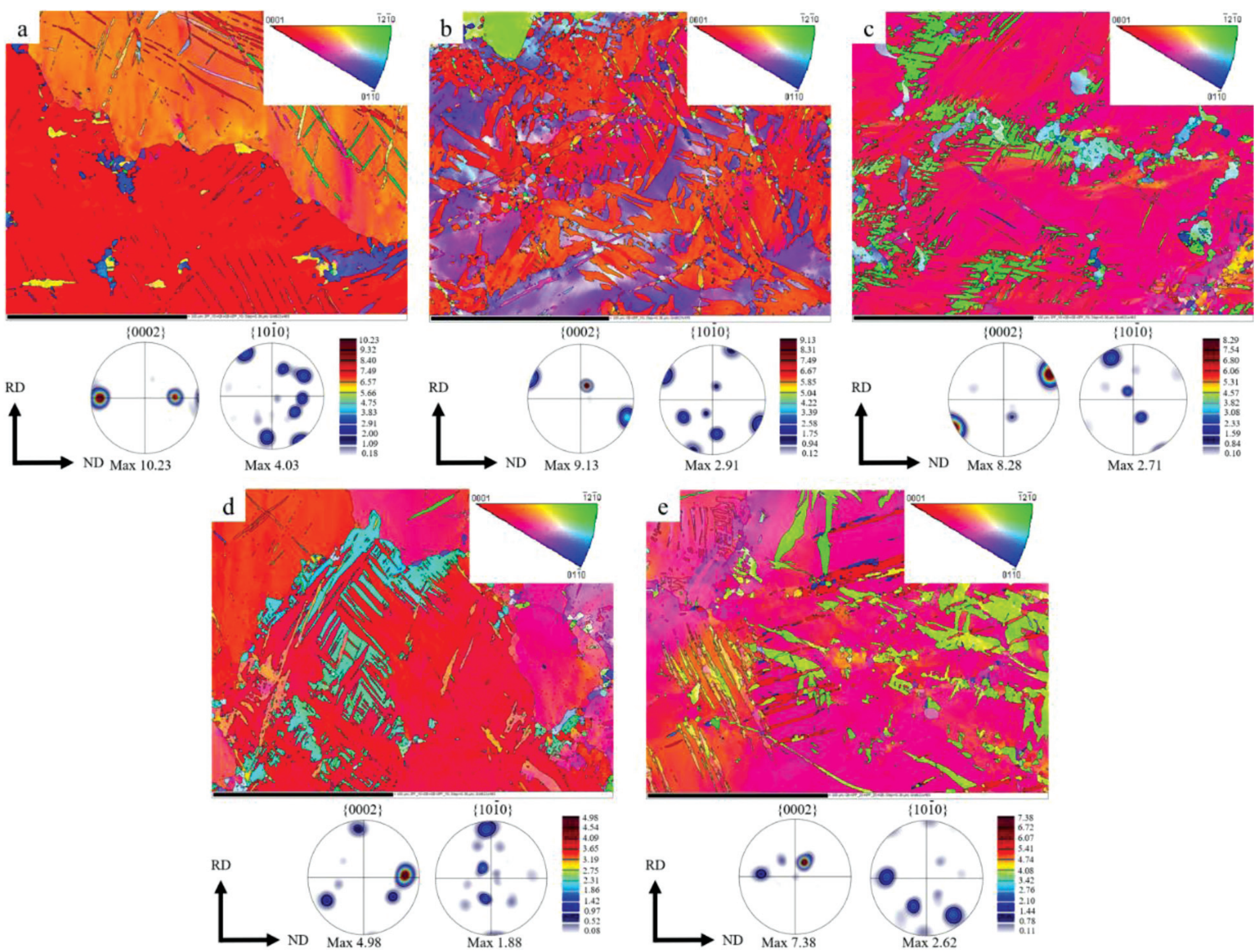

Figure 5: EBSD image and pole diagram of AZ91D magnesium alloy rolled by electric-pulse treatment at different output voltages: a) EP0 sample (0 V), b) EP1 sample (100 V), c) EP2 sample (200 V), d) EP3 sample (300 V), e) EP4 sample (400 V)

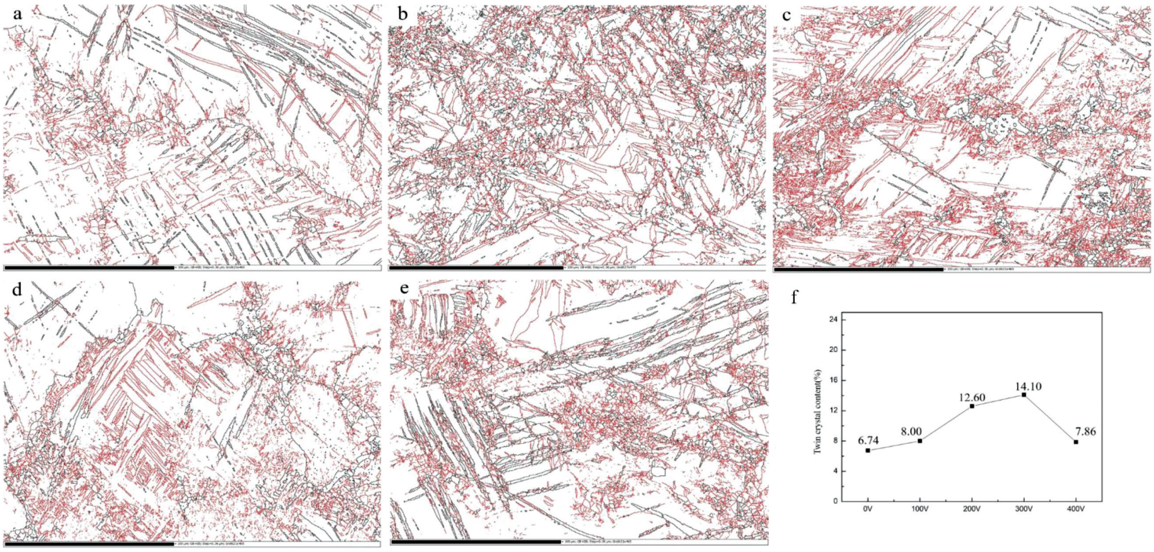

Figure 6: EBSD images of labeled twin grain boundaries of AZ91D magnesium alloy rolled by electric-pulse treatment at different output voltages: a) EP0 sample (0 V), b) EP1 sample (100 V), c) EP2 sample (200 V), d) EP3 sample (300 V), e) EP4 sample (400 V), f) twin content as a function of output voltage

nation between grains and optimizing the magnesium alloy weave.[23,24]

3.4 Effect of output voltage on electrical pulse AZ91D magnesium alloy twinning

The EBSD images of marked twin grain boundaries of the AZ91D magnesium alloy rolled by an electric pulse at different output voltages are shown in **Figure 6**. The red line indicates the $\{10\bar{1}2\}$ tensile twin grain boundaries, and the calculated statistics for twin content in the EP0-4 samples are presented in **Figure 6f**. It can be seen that the lowest twin content (6.74 %) occurred in the E0 sample where no electrical pulse was applied. The twin crystal content increased with increasing voltage, reaching a maximum of 14.10 % at 300 V, with a subsequent decrease to 7.86 % at 400 V.

The observed trend of an initial increase in twinning content up to 300 V followed and a decrease at 400 V indicates that the electric-pulse rolling has a promotional effect on the twinning of the AZ91D magnesium alloy samples that is optimum at 300 V. This increased twinning served to enhance the plastic-forming capability of AZ91D.

Increasing the output voltage in the range 0–300 V produces a Joule heating effect, and the increase in tem-

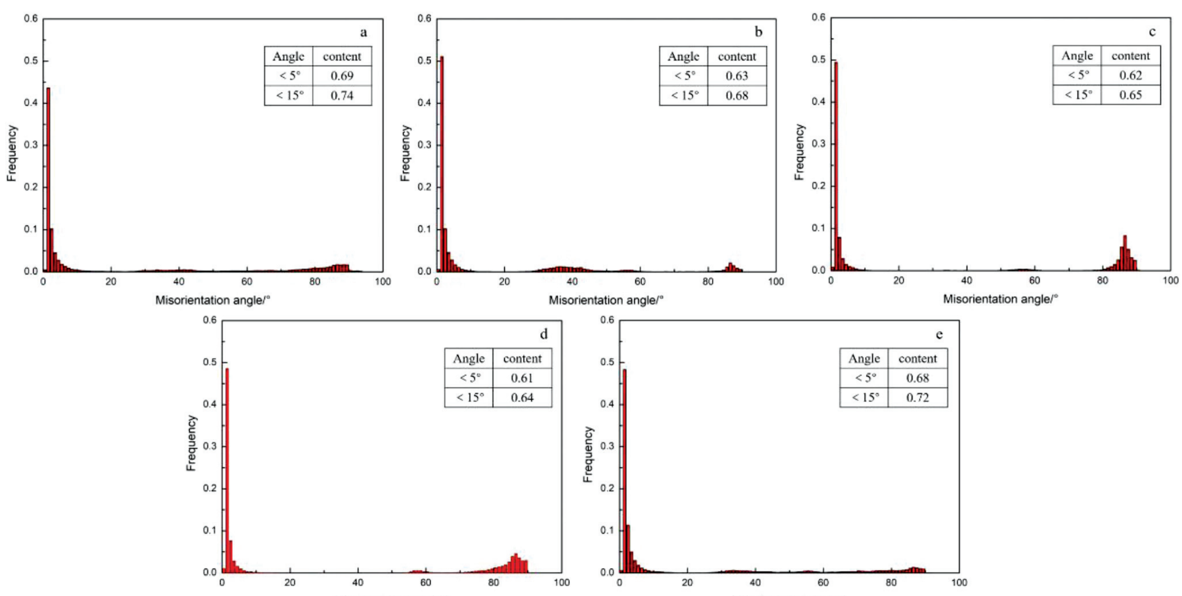

Figure 7: Distribution of misorientation angle in AZ91D magnesium alloy during electric-pulse rolling treatment under different output voltages: a) EP0 sample (0 V), b) EP1 sample (100 V), c) EP2 sample (200 V), d) EP3 sample (300 V), e) EP4 sample 400 V)

perature reduces the critical parting stress (CRSS) of the non-basal slip system of the magnesium alloy. More slip systems can then participate in plastic deformation with a resulting increase in the number of twins. When the voltage was increased to 400 V, the injection of excess energy caused the number of twins to decrease. This single-crystal orientation feature served to promote the migration of twin boundaries under cyclic stress, which led to changes in twin structure and even the disappearance of the twins.[25]

3.5 Effect of output voltage on the distribution of small-angle grain boundaries in AZ91D magnesium alloy rolled by electric-pulse treatment

The distribution of the grain-boundary angle orientation differences in the AZ91D magnesium alloy rolled by electric pulse at different output voltages is shown in **Figure 7**. The content of the small-angle grain boundaries < 5° in the EP0 sample was 69 %, with peaks appearing at ≈40° and ≈86°. At an output voltage of 100 V, the content of small-angle grain boundaries < 5° was lowered to 63%, and the peak at the ≈40° position was significantly enhanced, while the peak at the ≈86°position was less intense. When the output voltage was increased to 200 V, the content of small-angle grain boundaries < 5° was further lowered to 62 %, the peak at ≈40° position was negligible but the peak at ≈86 was enhanced. At an output voltage of 300 V, the content of small-angle grain boundaries < 5° fell to 61 %, the peak at ≈40° was no longer present, the peak at ≈86°was weakened, and a peak at ≈56° appeared. At an output voltage of 400 V, the content of small-angle grain boundaries < 5° increased to 68 %, the peak at ≈40° reappeared, and the peak at ≈86° showed a decrease in intensity.

With an increase of the output voltage, the content of small-angle grain boundaries < 5° in AZ91D first decreased, then increased and reached a minimum value at an output voltage of 300 V.

3.6 Effect of output voltage on the mechanical properties of AZ91D magnesium alloy rolled by electric-pulse treatment

3.6.1 Effect of output voltage on microhardness

The microhardness of each phase of AZ91D magnesium alloy rolled by electric-pulse treatment at different output voltages is illustrated in **Figure 8**. It can be seen that the α-Mg matrix and β-$Mg_{17}Al_{12}$ phase microhardness in EP0 are 58.8 HV and 98.8 HV, respectively. When the output voltage was increased to 100–300 V, the α-Mg matrix microhardness gradually decreased to give the lowest value (49.8 HV) at an output voltage of 300 V. The microhardness increased to 56.9 HV at an output voltage of 400 V. The microhardness of the β-$Mg_{17}Al_{12}$ phase gradually increased over the voltage range 100–200 V, giving the highest microhardness (118.8 HV) at 200 V. The microhardness subsequently decreased at an output voltage of 300–400 V to reach a microhardness of 101.7 HV at 400 V.

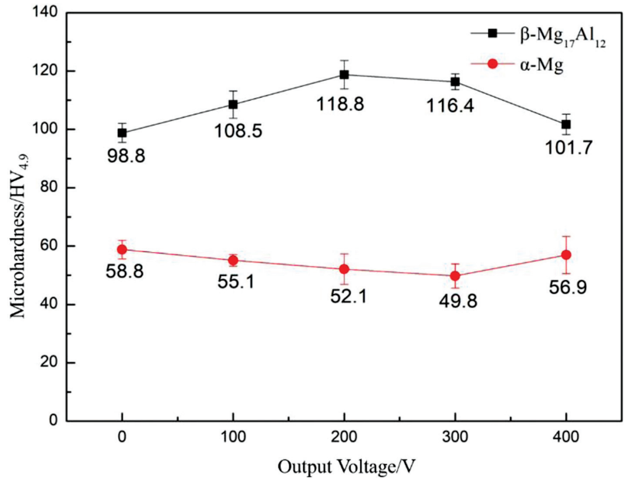

Figure 8: Microhardness of each phase in AZ91D magnesium alloy rolled by electric-pulse treatment at different output voltages

The electrical pulse treatment increases the diffusion rate of metal atoms, and high-energy pulse current results in an electron flow at high speed. This produces a high-frequency periodic impact effect on the atoms in the metal, resulting in a high-energy state that enhances the pulse-current non-thermal and Joule-heat effects.[21] The β-$Mg_{17}Al_{12}$ precipitated phase gradually solidifies into the α-Mg matrix at 0–200 V, the β-$Mg_{17}Al_{12}$ phase is refined and the α-Mg matrix solid solution is strengthened. The refinement and solid solution strengthening effect is more effective at an output voltage of 200V, leading to the highest observed AZ91D microhardness.

3.6.2 Effect of output voltage on tensile properties

The average tensile strength and elongation of the AZ91D are presented as a function of output voltage in **Figure 9**. In the voltage range 0–300 V, the tensile strength of the AZ91D increased to give a maximum ten-

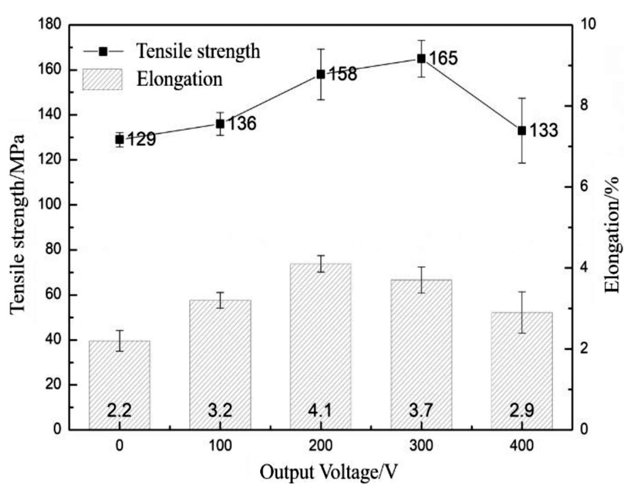

Figure 9: Tensile properties of AZ91D magnesium alloy rolled by electric pulse treatment at different output voltages

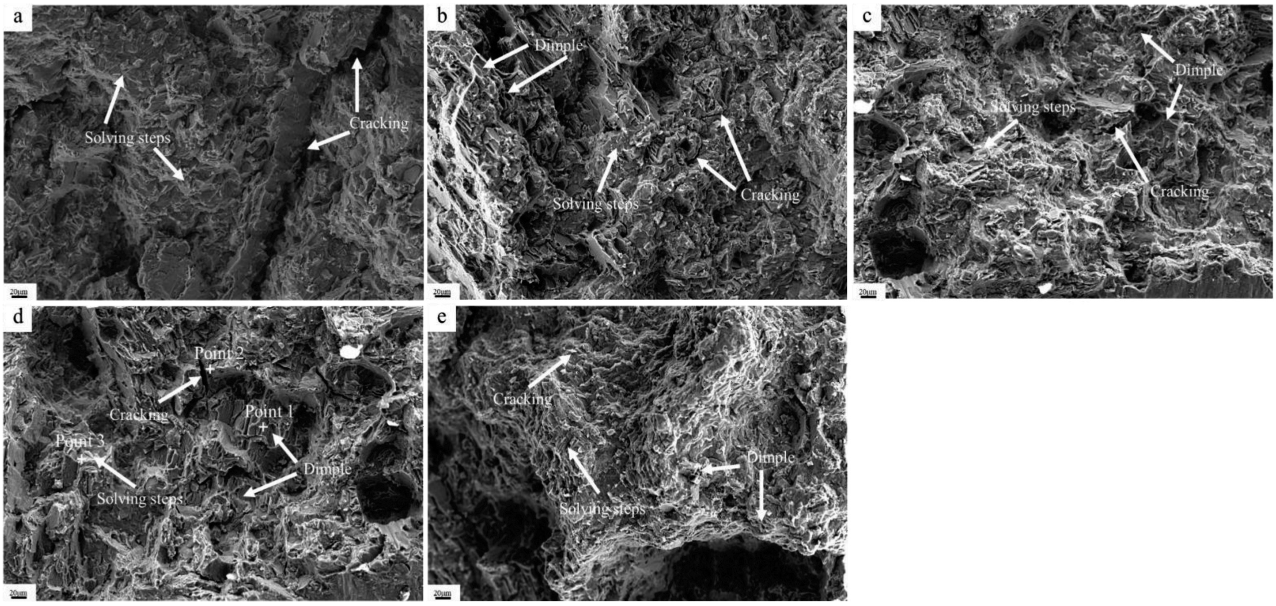

Figure 10: Fracture morphology of AZ91D magnesium alloy during electric-pulse rolling at different output voltages: a) EP0 sample (0 V), b) EP1 sample (100 V), c) EP2 sample (200 V), d) EP3 sample (300 V), e) EP4 sample (400 V)

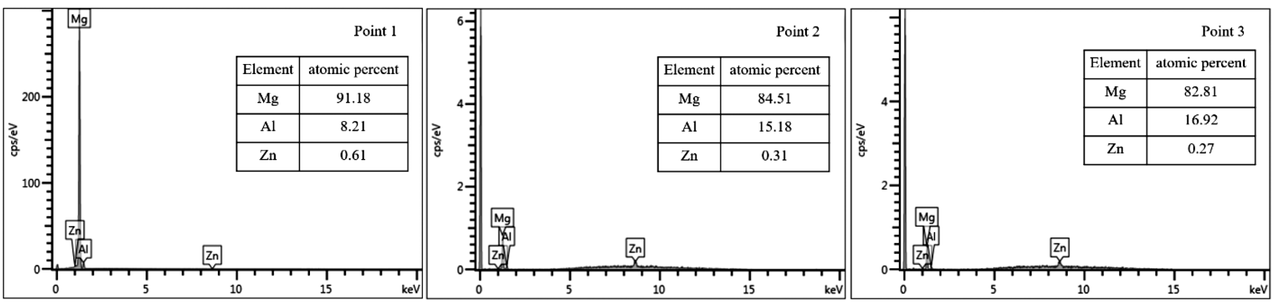

Figure 11: Energy spectrum analysis

sile strength of 165 MPa at 300 V. In the case of sample elongation, an increase was observed from 0 to 200 V, with a subsequent decrease in the voltage range 200–400 V. The highest elongation of electric-pulse-rolled AZ91D magnesium alloy samples was 4.1 % at an output voltage of 200 V. Combined with the SEM image analysis, it can be seen that when the pulse output voltage was 0–300 V, dissolution and refinement of the β-$Mg_{17}Al_{12}$ phase occurred in the magnesium alloy specimen, and the coarsening of the β-$Mg_{17}Al_{12}$ phase in the matrix served to increase the tensile strength.[26] At a pulse output voltage in the 0–200 V range, an appropriate electrical, thermal and stress energy was instantaneously transmitted to the material and the random thermal motion of the atoms generated sufficient kinetic energy to disrupt the equilibrium position with an enhanced diffusion of atoms and facilitated slipping and climbing of dislocations that extended elongation in AZ91D.[21]

The SEM images in **Figure 10** illustrate the fracture of the AZ91D magnesium alloy rolled by an electric pulse at different output voltages. When no electrical pulse was applied, there is clear evidence of cracks, destructive steps and some nest formations that demonstrate sample fracture. When the output voltage was increased, the tough nest in the fracture of AZ91D and the form of sample fracture changed from brittle to ductile fracture, with an accompanying improvement of plastic deformation. At a voltage of 200–400 V, the tough nest in the sample fracture decreased with a resultant poorer plastic-forming ability. According to the fixed-point energy-spectrum analysis, shown in **Figure 11**, the tough nests in the fracture were mainly distributed in the α-Mg matrix, while the cracks and deconstruction steps were mainly present in the β-$Mg_{17}Al_{12}$ phase and the α-Mg matrix, consistent with the analysis given above.

With an increase in the output voltage, the tensile strength and elongation of the AZ91D first increased and then decreased, reaching the highest tensile strength of 165 MPa at 300 V. The greatest elongation of the sample was 4.1 %, achieved at an output voltage of 200 V. From a consideration of the fracture analysis, an increased output voltage served to increase the tough nests in the fracture of AZ91D, most notably at 200 V. At a voltage in excess of 200 V, the tough nests were observed to decrease.

4 CONCLUSIONS

An increase in output voltage resulted in greater sample surface cracking, and the best surface quality was achieved at an output voltage of 300 V. The lowest content of β-$Mg_{17}Al_{12}$ phase in the sample was 8.4% at an output voltage of 300 V.

At an output voltage of 300 V, the samples exhibited the lowest weave strength on {0002} and $\{10\bar{1}0\}$, the greatest degree of twinning, and the best plastic-forming ability.

The microhardness of the β-$Mg_{17}Al_{12}$ phase was highest at an output voltage of 200 V, and the microhardness of the α-Mg matrix was lowest at an output voltage of 300 V. The maximum tensile strength of the sample was 165 MPa at an output voltage of 300 V. Moreover, the maximum sample elongation was 4.1% at an output voltage of 200 V.

Acknowledgement

Supported by the National Natural Science Foundation of China (52061002)

Ningxia Hui Autonomous Region Key R&D Program (2023BDE03007)

Graduate Innovation Project of North Minzu University (YCX23108)

5 REFERENCES

[1] W. Li, K. Deng, X. Zhang, C. Wang, J. Kang, K. Nie, W. Liang, Microstructures, tensile properties and work hardening behavior of Si-Cp/Mg-Zn-Ca composites, Journal of Alloys and Compounds, 695 (**2016**) 2215–2223, doi:10.1016/j.jallcom.2016.11.070

[2] K. Edalati, R. Uehiro, Y. Ikeda, H. Li, H. Emami, Y. Filinchuk, Z. Horita, Design and synthesis of a magnesium alloy for room temperature hydrogen storage, Acta Materialia, 149 (**2018**) 88–96, doi:10.1016/j.actamat.2018.02.033

[3] B. Yan, K. Deng, J. Kang, Mechanical and wear resistance properties of (Grp+SiCp)/AZ91 mag-nesium matrix composites, Rare Metal Materials and Engineering, 48 (**2019**) 2251–2257, doi:10.3390/ma12071190

[4] Y. Liu, Study on the microplastic deformation behavior of TA2 pure titanium assisted by electric- current, Harbin, Harbin Institute of Technology, 1 (**2015**) 10–12, doi:10.7666/d.D754107

[5] Z. Zhao, G. Wang, H. Hou, Y. Zhang, Y. Wang, Effect of pulsed current on the deformation behavior of 0.27% hydrogen-substituted Ti-6Al-4V alloy, Journal of Materials Research, 5 (**2018**) 321–326, doi:10.1038/s41598-018-32857-6

[6] O. Troitskiy, V. Stashenko, Electroplastic wire drawing: A promising method of production of lightweight wire and cable, Journal of Machinery Manufacture and Reliability, 44 (**2015**) 758–765, doi:10.3103/S1052618815080087

[7] K. Yao, J. Wang, M. Zheng, A research on electroplastic effects in wire-drawing process of an austenitic stainless steel, Scripta Materialia, 45 (**2001**) 533–539, doi:10.1016/S1359-6462(01)01054-5

[8] W. Salandro, C. Bunget, L. Mears, Modeling and Quantification of the Electroplastic Effect When Bending Stainless Steel Sheet Metal//Asme International Manufacturing Science & Engineering Conference, 32 (**2010**) 591–590

[9] A. Jordan, B. Kinsey, Investigation of thermal and mechanical effects during electrically-assisted microbending, Journal of Materials Processing Technology, 221 (**2015**) 1–12, doi:10.1016/j.jmatprotec.2015.01.021

[10] M. Yoo, Slip, twinning, and fracture in hexagonal close-packed metals, Metallurgical Transactions A, 12 (**1981**) 409–418, doi:10.1007/bf02648537

[11] H. Huang, Study of plastic deformation mechanism and recrystallization behavior of AZ31 magnesium alloy, Thesis, Qinghua University, Beijing, 2014

[12] S. Agnew, C. Tomé, D. Brown, T. Holden, S. Vogel, Study of slip mechanisms in a magnesium alloy by neutron diffraction and modeling, Scripta Materialia, 48 (**2003**) 1003–1008, doi:10.1016/S1359-6462(02)00591-2

[13] Y. Zhou, W. Zhang, B. Wang, G. He, J. Guo, Grain refinement and formation of ultrafine-grained microstructure in a low-carbon steel under electropulsing, Journal of Materials Research, 17 (**2002**) 2105–2111, doi:10.1557/JMR.2002.0311

[14] Y. Zhou, S. Xiao, J. Guo, Recrystallized microstructure in cold worked brass produced by electropulsing treatment, Materials Letters, 58 (**2004**) 1948–1951, doi:10.1016/j.matlet.2003.11.035

[15] X. Wang, W. Dai, C. Ma, X. Zhao, Effect of electric current direction on recrystallization rate and texture of a Cu-Zn alloy, Journal of Materials Research, 28 (**2013**) 1378–1385, doi:10.1557/jmr.2013.86

[16] X. Wang, M. Liu, W. Dai, N. Wu, X. Zhao, Effect of electric current direction on the microstructural evolution and mechanical properties of a cold-rolled Cu–Zn alloy during the phase transformation induced by electric current pulses, Journal of Materials Research, 30 (**2015**) 2500–2507, doi:10.1557/jmr.2015.226

[17] H. Zhang, Y. Liu, H. Dong, B. Jin, J. Fan, Microstructure, mechanical properties and static recrystallization behavior of the rolled ZK60 magnesium alloy sheets processed by electropulsing treatment, Journal of Alloys & Compounds, 646 (**2015**) 1–9, doi:10.1016/j.jallcom.2015.04.196

[18] Y. Liu, J. Fan, H. Zhang, W. Jin, H. Dong, B. Xu, Recrystallization and microstructure evolution of the rolled Mg-3Al-1Zn alloy strips under electropulsing treatment, Journal of Alloys & Compounds, 622 (**2015**) 229–235, doi:10.1016/j.jallcom.2014.10.062

[19] H. Jeong, M. Kim, J. Park, C. Yim, J. Kim, O. Kwon, P. Madakashira, H. Han, Effect of pulsed electric current on dissolution of $Mg_{17}Al_{12}$ phases in as-extruded AZ91 magnesium alloy, Materials Science & Engineering A, 684 (**2017**) 668–676, doi:10.1016/j.msea.2016.12.103

[20] I. Indhiarto, T. Shimizu, M. Yang, Effect of Peak Current Density on Tensile Properties of AZ31B Magnesium Alloy, Materials, 14 (**2021**) 1457, doi:10.3390/ma14061457

[21] C. Han, Study on the mechanism of action of high-energy electric pulse toughening of alloy steel, University of Science and Technology Beijing, **2023**, doi:10.26945/d.cnki.gbjku.2023.000043

[22] L. Zhang, Y. Li, Research progress on grain refinement methods for magnesium alloys, Foundry, 68 (**2019**) 1195–1203, doi:10.3390/met12081388

[23] M. Yuasa, N. Miyazawa, M. Hayashi, M. Mabuchi, Y. Chino, Effects of group II elements on the cold stretch formability of Mg-Zn alloys, Acta Materialia, 83 (**2015**) 294–303, doi:10.1016/j.actamat.2014.10.005

[24] Y. Tang, W. Huo, L. Dong, W. Zhang, H. Peng, S. Zhang, An ultra-high formability at room temperature induced by continually dynamic micro-nanocrystallization of Mg rare earth alloy, Materials Letters, 339 (**2023**) 134090, doi:10.1016/j.matlet.2023.134090

[25] H. Qiao, S. Agnew, P. Wu, Modeling twinning and detwinning behavior of Mg alloy ZK60A during monotonic and cyclic loading, International Journal of Plasticity, 65 (**2015**) 61–84, doi:10.1016/j.ijplas.2014.08.010

[26] Z. Shan, Microstructure and mechanical properties of AZ-system deformed magnesium alloy treated with high-density pulse current, Taiyuan University of Technology, **2022**, doi:10.27352/d.cnki.gylgu.2020.002013